

# Optical ranging with quantum advantage

Sankar Davuluri<sup>\*1</sup>, Greeshma Gopinath<sup>1</sup> and Matt J. Woolley<sup>2</sup>

<sup>1</sup>*BITS Pilani, Hyderabad Campus, 500078, India*

<sup>2</sup>*School of Engineering and Technology, UNSW Canberra, Canberra, Australian Capital Territory, Australia.*

<sup>\*</sup>sankar@hyderabad.bits-pilani.ac.in

October 31, 2023

**abstract** The quantum illumination technique requires joint measurement between the idler and the probe reflected from the low-reflective target present in a noisy environment. The joint measurement is only possible with prior knowledge about the target's location. The technique in this article overcomes this limitation by using entanglement and a cross-correlated homodyne measurement. This technique does not require quantum storage of the idler and prior knowledge about the target's distance. The cross-correlation measurement makes this technique completely immune to environmental noise, as the correlation between the idler and the environment is zero. The low reflectivity of the target is negated by increasing the intensity of the reference fields (non-entangled) in the homodyne. Based on heuristic arguments, a lower bound of the target's reflectivity for optimum application of this technique is described.

## 1 Introduction

Quantum illumination (QI) [1, 2, 3] has shown that entangled photons can detect the presence of a low reflective target in a noisy background more efficiently than non-entangled photons. The QI protocol is studied using different quantum states like Gaussian states [4, 5, 6], discrete [7] and continuous variable entanglement [8, 9], cat states [10], photon number entangled states [11],  $N$ -photon entangled states [12], and hyper-entanglement [13]. There have been several studies [14, 15, 16] about optimum detection schemes like parametrically amplified idler [17] and double homodyne [18]. A remarkable feature of QI is that the residual quantum correlations [19, 20] between the probe and the idler will provide a quantum advantage even after losing the entanglement because of the environment [21, 22, 23]. The QI technique is extended to microwave frequencies theoretically [24] and experimentally [25, 26, 27, 35]. Recently, QI has used the quantum eraser concept to make it immune to jamming [28] by detecting only the locally stored reference fields. The robustness of QI to environment and background noise makes it particularly useful for radar technology. However, QI detection of the low-reflective target in different locations requires appropriately readjusting the idler storage times for each location. If the location of the low-reflective target is unknown, storing the idler exactly until the probe's return is impossible. This limits the application of QI from full-ranging applications like lidar and radar. The lack

of quantum ranging function has limited QI to imaging in some studies [29]. Nevertheless, QI unquestionably outperforms [30, 31, 32, 33] the classical detection strategies in noisy environments. Hence, the QI has been modified into several versions, discussed in the next paragraph, to build a quantum radar or lidar.

Digitization technique [25, 34, 26, 35] circumvents the quantum storage of idler by measuring the signal and probe independently. The measured data is post-processed to complete the QI protocol digitally [25]. This method can not add ranging functionality because joint measurement of idler and signal photons in the digitized version is required. The authors in Ref. [26, 35] studied quantum noise correlated radar. Their experiment introduced quantum noise correlations using entanglement but did not use a low-reflective target for detection and ranging. Instead, their experiment showed entanglement enhanced detection of microwaves in a noisy environment. Later studies [36, 37] included a target, but these studies switched to photon coincidence detection, which requires prior knowledge about the target's location. There have been several theoretical proposals [38, 39, 40, 41] to overcome the range and/or velocity limitation of QI protocol and to study the quantum limits [42, 3, 43]. Multiary hypothesis testing added ranging functionality to QI by dividing the entire range into multiple blocks [40]; however, an optimum detection scheme for a range with blocks more than two remains an open question. Quantum localization is studied [38] to add ranging function to QI; however, the  $N$  photon entangled probes are highly sensitive to decoherence [44] and achieving entangled states with  $N > 2$  is quite challenging. The quantum-enhanced Doppler lidar [39] can provide information about the target's velocity but not distance.

In this paper, we propose combining QI with a cross-correlated homodyne detection scheme using digitization [25, 34, 26, 35]. This technique offers the following advantages compared to the standard quantum illumination technique. (i) Quantum storage of the idler field and prior knowledge about the distance of the low-reflective target are not required. (ii) Target detection and ranging efficiency are independent of entangled field intensity and environmental noise. (iii) The low-reflectivity property of the target can be negated by increasing the intensity of the reference fields (non-entangled) in the homodyne.

## 2 Quantum illumination with homodyne cross-correlation

Figure 1 shows the schematics of the system under study. Destruction operators of each entangled are represented with  $\hat{B}$  and  $\hat{D}$  as shown in Fig. (1). The  $\hat{D}$  field mixes with a reference field, represented with destruction operator  $\hat{D}_1$ , in the homodyne-3 setup shown in Fig. (1). Then the difference in intensities is given as

$$\hat{I}_4 - \hat{I}_3 \approx 2\sqrt{I_D I_{D_1}} \sin \phi_1 + [\cos \phi_1 (\sqrt{I} \hat{Y}_D - \sqrt{I_D} \hat{Y}_{D_1}) + \sin \phi_1 (\sqrt{I} \hat{X}_D + \sqrt{I_D} \hat{X}_{D_1})], \quad (1)$$

where  $\phi_1$  is the phase difference between  $\hat{D}$  and  $\hat{D}_1$ ,  $\hat{Y}_O = i(\hat{\delta}_O^\dagger - \hat{\delta}_O)$ ,  $\hat{X}_O = \hat{\delta}_O^\dagger + \hat{\delta}_O$  with  $\hat{\delta}_O$  as the quantum fluctuation and  $\bar{O}$  as the classical mean of operator  $\hat{O}$  ( $O = B, D, D_1$ ),  $I_D = \langle \hat{D}^\dagger \hat{D} \rangle$  and  $I = \langle \hat{D}_1^\dagger \hat{D}_1 \rangle$ . The suffix ‘ $\dagger$ ’ represents an adjoint operation. All the optical operators  $\hat{B}$ ,  $\hat{D}$ , and  $\hat{D}_1$  are normalized such that  $I$  and  $I_D$  represent the number of photons per unit time. By tuning the  $\hat{D}_1$  phase, we set  $\phi_1 = \pi/2$ . Then the linearized quantum fluctuation  $\hat{\theta}_D$  in Eq. (1) is given as

$$\hat{\theta}_D(t) = [\sqrt{I} \hat{X}_D(t) + \sqrt{I_D} \hat{X}_{D_1}(t)], \quad (2)$$

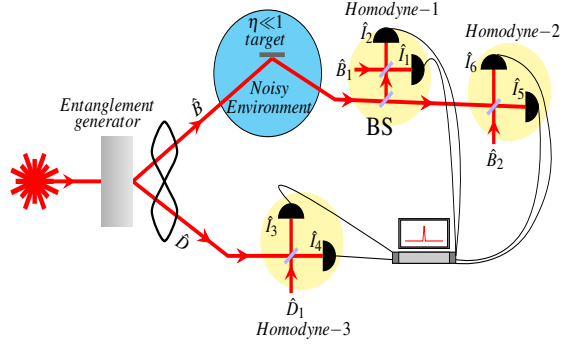


Figure 1: Quantum illumination with cross-correlated homodyne.  $\hat{B}$  and  $\hat{D}$  are the destruction operators for the entangled fields.  $\hat{B}_1$ ,  $\hat{B}_2$ , and  $\hat{D}_1$  are destruction operators for the reference fields in homodyne setups.  $\hat{I}_i$  ( $i = 1, 2, \dots, 6$ ) are intensities at the photo detectors. BS is a beam splitter.

where  $t$  is the time. Showing the  $t$  dependence explicitly in Eq. (2) will be useful later in this draft.

On the other hand,  $\hat{B}$  is sent into the environment to probe the presence of a low reflective  $\eta \ll 1$  target. A tiny amount of  $\hat{B}$  will be received if the low reflective target is present; otherwise, only the environmental noise will be received. The received signal is given as  $\sqrt{\eta}\hat{B}e^{i\phi_B} + \sqrt{1-\eta}\hat{E}$ , where  $\hat{E}$  and  $\phi_B$  are the destruction operator of the environment and phase acquired by  $\hat{B}$  as it travels through the unknown path in the environment, respectively. This signal is then split into two parts using the beam splitter BS as shown in Fig. (1). One part mixes with a reference field  $\hat{B}_2e^{i\phi_2}$ , where  $\phi_2$  and  $\hat{B}_2$  are the phase and destruction operator of the reference field, in homodyne-2 (see the Fig. (1)). Then the difference in intensities at the photodetectors is given as

$$\begin{aligned} \hat{I}_5 - \hat{I}_6 = & i\sqrt{\frac{\eta}{2}}(\hat{B}^\dagger\hat{B}_2e^{-i\phi} - \hat{B}_2^\dagger\hat{B}e^{i\phi}) + i\sqrt{\frac{1-\eta}{2}}(\hat{E}^\dagger\hat{B}_2e^{i\phi_2} - \hat{B}_2^\dagger\hat{E}e^{-i\phi_2}) \\ & + \sqrt{\frac{1}{2}}(\hat{V}^\dagger\hat{B}_2e^{i\phi_2} + \hat{B}_2^\dagger\hat{V}e^{-i\phi_2}), \end{aligned} \quad (3)$$

where  $\phi = \phi_B - \phi_2$ , the superfix ‘\*’ represents complex conjugate, and  $\hat{V}$  is the destruction operator for the vacuum field entering through the empty port of BS. By writing  $\hat{B}_2$  as sum of its classical mean  $\bar{B}_2$  and quantum fluctuation  $\delta_{B_2}$ , the linearized fluctuation  $\hat{\theta}_{B_2}$  in Eq. (3) is given as

$$\begin{aligned} \hat{\theta}_{B_2}(t_1) = & \sqrt{\frac{\eta}{2}}\{[\cos\phi[\sqrt{I}\hat{Y}_B(t_1) - \sqrt{I_B}\hat{Y}_{B_2}(t_1)] + \sin\phi[\sqrt{I}\hat{X}_B(t_1) + \sqrt{I_B}\hat{X}_{B_2}(t_1)]]\} + \\ & i\sqrt{\frac{(1-\eta)I}{2}}[\hat{E}^\dagger(t_1)e^{i\phi_2} - e^{-i\phi_2}\hat{E}(t_1)] + \sqrt{\frac{I}{2}}[\hat{V}^\dagger(t_1)e^{i\phi_2} + e^{-i\phi_2}\hat{V}(t_1)], \end{aligned} \quad (4)$$

where  $I_B = \langle \hat{B}^\dagger\hat{B} \rangle$  and we set  $\langle \hat{B}_2^\dagger\hat{B}_2 \rangle = I$ . The reflected field from the BS mixes with another reference field, with destruction operator  $\hat{B}_1$  and phase  $\phi_2$ , in homodyne-1. The  $\hat{B}_1$  is phase-locked with  $\hat{B}_2$ , so both have the same phase  $\phi_2$ . The optical path lengths

from the BS to *homodyne* – 1 and *homodyne* – 2 are adjusted to be equal. Then the difference in intensities at the photo-detectors is

$$\hat{I}_2 - \hat{I}_1 = \sqrt{\frac{\eta}{2}}(\hat{B}^\dagger \hat{B}_1 e^{-i\phi} + \hat{B}_1^\dagger \hat{B} e^{i\phi}) + \sqrt{\frac{1-\eta}{2}}(\hat{E}^\dagger \hat{B}_1 e^{i\phi_2} + \hat{B}_1^\dagger e^{-i\phi_2} \hat{E}) + i\sqrt{\frac{1}{2}}(\hat{V}^\dagger \hat{B}_1 e^{i\phi_2} - \hat{B}_1^\dagger e^{-i\phi_2} \hat{V}). \quad (5)$$

After writing  $\hat{B}_1$  as sum of its mean  $\bar{B}_1$  and quantum fluctuation  $\hat{\delta}_{B_1}$ , the linearized fluctuation  $\hat{\theta}_{B_1}$  in Eq. (5) is

$$\hat{\theta}_{B_1}(t_1) = \sqrt{\frac{\eta}{2}}\{-\sin\phi[\sqrt{I}\hat{Y}_B(t_1) - \sqrt{I_B}\hat{Y}_{B_1}(t_1)] + \cos\phi[\sqrt{I}\hat{X}_B(t_1) + \sqrt{I_B}\hat{X}_{B_1}(t_1)]\} + \sqrt{\frac{(1-\eta)I}{2}}[\hat{E}^\dagger(t_1)e^{i\phi_2} + e^{-i\phi_2}\hat{E}(t_1)] + i\sqrt{\frac{I}{2}}[\hat{V}^\dagger(t_1)e^{i\phi_2} - e^{-i\phi_2}\hat{V}(t_1)], \quad (6)$$

where  $\bar{B}_1$  is the mean value of  $\hat{B}_1$ , and we set  $\langle \hat{B}_1^\dagger \hat{B}_1 \rangle = I$ . Note the phase difference is  $\phi$  in both Eq. (6) and Eq. (4) as  $\hat{B}_1$  and  $\hat{B}_2$  are phase-locked to have the same phase. Using Eq. (1), Eq. (6) and Eq. (4), we can write

$$\langle \hat{\theta}_D(t) \hat{\theta}_{B_2}(t_1) \rangle = \sqrt{\frac{\eta}{2}}I^2[\cos\phi \langle \hat{X}_D(t) \hat{Y}_B(t_1) \rangle + \sin\phi \langle \hat{X}_D(t) \hat{X}_B(t_1) \rangle], \quad (7)$$

$$\langle \hat{\theta}_D(t) \hat{\theta}_{B_1}(t_1) \rangle = \sqrt{\frac{\eta}{2}}I^2[-\sin\phi \langle \hat{X}_D(t) \hat{Y}_B(t_1) \rangle + \cos\phi \langle \hat{X}_D(t) \hat{X}_B(t_1) \rangle], \quad (8)$$

where  $\langle \hat{O}_1 \hat{O}_2 \rangle = \langle \hat{O}_1 \hat{O}_2 + \hat{O}_2 \hat{O}_1 \rangle / 2$  is the symmetrization operation with  $\hat{O}_1 = \hat{\theta}_D, \hat{X}_D, \hat{Y}_D$  and  $\hat{O}_2 = \hat{\theta}_{B_1}, \hat{\theta}_{B_2}, \hat{Y}_B, \hat{X}_B$ . Note that the cross-correlations in Eq. (8) and Eq. (7) are immune to environmental noise. The Eq. (8) and Eq. (7) can be non-zero only if  $\hat{B}$  and  $\hat{D}$  are quantum correlated. A non-zero value for Eq. (8) and Eq. (7) establishes the presence of the low-reflective target. The  $\phi$  in Eq. (8) and Eq. (7) is an unknown variable as the exact trajectory of  $\hat{B}$  is unknown. The  $\phi$  dependence can be eliminated from Eq. (8) and Eq. (7) by rewriting them as

$$\langle \hat{\theta}_D(t) \hat{\theta}_{B_1}(t_1) \rangle^2 + \langle \hat{\theta}_D(t) \hat{\theta}_{B_2}(t_1) \rangle^2 = \frac{\eta}{2}I^2[\langle \hat{X}_D(t) \hat{Y}_B(t_1) \rangle^2 + \langle \hat{X}_D(t) \hat{X}_B(t_1) \rangle^2]. \quad (9)$$

Measurement of cross-correlations such as in Eq. (9) is discussed in Ref. [45]. The  $\hat{X}$  and  $\hat{Y}$  quadratures of the signal and idler fields are proportional to the voltage quadratures in the homodyne [25, 35] measurement. The Eq. (9) is evaluated by scanning the pre-recorded homodyne-3 measurement against the homodyne-1 and homodyne-2 measurement records. As  $\langle \hat{X}_B(t) \hat{Y}_D(t_1) \rangle \propto \delta(t - t_1)$ , a non-zero value for Eq. (9) implies that the distance of the low-reflective target is  $(t - t_1)c/2$ . We assumed that the low-reflective object is equidistant from the receiver and sender and  $c$  is the velocity of light.

Generally, the  $\eta$  of a non-cooperative target is not known and is very small. The small value of  $\eta$  in Eq. (9) can be compensated by increasing the intensity of the reference fields in the homodynes. It is possible to set  $I \gg 1$  so that the product  $\eta I^2 \geq 2$  for  $\eta \ll 1$  in Eq. (9). If the correlation in Eq. (9) is greater than or equal to  $\langle \hat{Y}_D(t) \hat{Y}_B(t_1) \rangle^2 + \langle \hat{Y}_D(t) \hat{X}_B(t_1) \rangle^2$ , the presence of a target with  $\eta \geq 2/I^2$  can be confirmed and its distance can be measured. Hence, it is safe to claim that the technique described in this work can detect and range targets with  $\eta \geq 2/I^2$ .

## 2.1 Optimization

The correlations in Eq. (9) are dependent on  $\hat{X}_D$  (not  $\hat{Y}_D$ ) as  $\phi_1 = \pi/2$  in Eq. (1). For  $\phi_1 \neq 0$ , Eq. (7) and Eq. (8) has to be rewritten as

$$\begin{aligned} \langle \overline{\hat{\theta}_D(t) \hat{\theta}_{B2}(t_1)} \rangle &= \sqrt{\frac{\eta I^2}{2}} [\cos \phi \cos \phi_1 \langle \overline{\hat{Y}_D(t) \hat{Y}_B(t_1)} \rangle + \sin \phi \cos \phi_1 \langle \overline{\hat{Y}_D(t) \hat{X}_B(t_1)} \rangle \\ &\quad + \sin \phi_1 \cos \phi \langle \overline{\hat{X}_D(t) \hat{Y}_B(t_1)} \rangle + \sin \phi_1 \sin \phi \langle \overline{\hat{X}_D(t) \hat{X}_B(t_1)} \rangle], \end{aligned} \quad (10)$$

$$\begin{aligned} \langle \overline{\hat{\theta}_D(t) \hat{\theta}_{B1}(t_1)} \rangle &= \sqrt{\frac{\eta I^2}{2}} [-\sin \phi \cos \phi_1 \langle \overline{\hat{Y}_D(t) \hat{Y}_B(t_1)} \rangle + \cos \phi \cos \phi_1 \langle \overline{\hat{Y}_D(t) \hat{X}_B(t_1)} \rangle \\ &\quad - \sin \phi \sin \phi_1 \langle \overline{\hat{X}_D(t) \hat{Y}_B(t_1)} \rangle + \sin \phi_1 \cos \phi \langle \overline{\hat{X}_D(t) \hat{X}_B(t_1)} \rangle]. \end{aligned} \quad (11)$$

Using Eq. (10) and Eq. (11), we can write

$$\begin{aligned} \langle \overline{\hat{\theta}_D(t) \hat{\theta}_{B1}(t_1)} \rangle^2 + \langle \overline{\hat{\theta}_D(t) \hat{\theta}_{B2}(t_1)} \rangle^2 &= \{ [\langle \overline{\hat{Y}_D(t) \hat{Y}_B(t_1)} \rangle^2 + \langle \overline{\hat{Y}_D(t) \hat{X}_B(t_1)} \rangle^2] \cos^2 \phi_1 \\ &\quad + [\langle \overline{\hat{X}_D(t) \hat{Y}_B(t_1)} \rangle^2 + \langle \overline{\hat{X}_D(t) \hat{X}_B(t_1)} \rangle^2] \sin^2 \phi_1 \\ &\quad + [\langle \overline{\hat{Y}_D(t) \hat{Y}_B(t_1)} \rangle \langle \overline{\hat{X}_D(t) \hat{Y}_B(t_1)} \rangle + \langle \overline{\hat{Y}_D(t) \hat{X}_B(t_1)} \rangle \langle \overline{\hat{X}_D(t) \hat{X}_B(t_1)} \rangle] \sin(2\phi_1) \} \frac{\eta}{2} I^2. \end{aligned} \quad (12)$$

Setting  $\phi_1 = \pi/2$  reduces Eq. (12) into Eq. (2) as expected. By adjusting the phase  $\phi = 0$ , we can rewrite Eq. (12) as

$$\langle \overline{\hat{\theta}_D(t) \hat{\theta}_{B1}(t_1)} \rangle^2 + \langle \overline{\hat{\theta}_D(t) \hat{\theta}_{B2}(t_1)} \rangle^2 = \frac{\eta}{2} I^2 [\langle \overline{\hat{Y}_D(t) \hat{Y}_B(t_1)} \rangle^2 + \langle \overline{\hat{Y}_D(t) \hat{X}_B(t_1)} \rangle^2]. \quad (13)$$

The Eq. (12) is a more general relation for any arbitrary  $\phi_1$ . The Eq. (13) and Eq. (9) prove that the cross-correlation of homodyne-3 with homodyne-1 and homodyne-2 can be tuned to be a function of maximum possible correlations by tuning  $\phi_1$ . At this point, it is impossible to say which correlations will give maximum value as it depends on the entanglement generation mechanism. For example, some entanglement schemes [46] exhibit stronger  $\langle \hat{Y}_D \hat{Y}_B \rangle$  correlation in which case  $\phi_1 = 0$  (or Eq. (13)) is the optimized detection scheme. Whereas, a two-mode squeezed coherent state exhibit equal correlation strength for both  $\langle \hat{X}_D \hat{X}_B \rangle$  and  $\langle \hat{Y}_D \hat{X}_B \rangle$  and hence either Eq. (13) or Eq. (9) will provide an optimum result.

## 2.2 Quantum advantage

The quantum advantage of this technique can be estimated by comparing it with the corresponding classical system. The corresponding classical system is built by replacing the quantum fields  $\hat{B}$  and  $\hat{D}$  with classical field amplitudes  $\tilde{B}$  and  $\tilde{D}$ , respectively. The classical field amplitudes are normalized such that  $|\tilde{B}|^2 = \tilde{I}_B$  and  $|\tilde{D}|^2 = \tilde{I}_D$  with  $\tilde{I}_B$  and  $\tilde{I}_D$  as the classical field intensities, respectively. Adding an identical random phase fluctuation  $\tilde{\delta}(t)$  to both  $\tilde{B}$  and  $\tilde{D}$  introduces correlation in the classical system. Now the fluctuation  $\tilde{\theta}_D$  in the output from the homodyne-3 is given as

$$\tilde{\theta}_D = \sqrt{\tilde{I}_D} \sin \tilde{\delta}(t) \approx \sqrt{\tilde{I}_D} \tilde{\delta}(t), \quad (14)$$

for  $\tilde{\delta}(t) < 1$ . Similarly, the fluctuation  $\tilde{\theta}_{B1}$  ( $\tilde{\theta}_{B1}$ ) in the output from homodyne-1 (homodyne-2) is given as

$$\begin{aligned} \tilde{\theta}_{B1}(t_1) = & \sqrt{\frac{\eta}{2}}[-\sin\phi\sqrt{I\tilde{I}_B}\tilde{\delta}(t_1)] + \sqrt{\frac{(1-\eta)I}{2}}[\hat{E}^\dagger(t_1)e^{i\phi_2} + e^{-i\phi_2}\hat{E}(t_1)] \\ & + i\sqrt{\frac{I}{2}}[\hat{V}^\dagger(t_1)e^{i\phi_2} - e^{-i\phi_2}\hat{V}(t_1)], \end{aligned} \quad (15)$$

$$\begin{aligned} \tilde{\theta}_{B2}(t_1) = & \sqrt{\frac{\eta}{2}}[\cos\phi\sqrt{I\tilde{I}_B}\tilde{\delta}(t_1)] + i\sqrt{\frac{(1-\eta)I}{2}}[\hat{E}^\dagger(t_1)e^{i\phi_2} - e^{-i\phi_2}\hat{E}(t_1)] \\ & + \sqrt{\frac{I}{2}}[\hat{V}^\dagger(t_1)e^{i\phi_2} + e^{-i\phi_2}\hat{V}(t_1)]. \end{aligned} \quad (16)$$

Using Eq. (14), Eq. (15), and Eq. (16), the best performance of the classical system is given as

$$\langle\tilde{\theta}_D(t)\tilde{\theta}_{B1}(t_1)\rangle^2 + \langle\tilde{\theta}_D(t)\tilde{\theta}_{B2}(t_1)\rangle^2 = \frac{\eta}{2}I^2\tilde{I}_D\tilde{I}_B[\langle\tilde{\delta}(t)\tilde{\delta}(t_1)\rangle]^2. \quad (17)$$

To compare the classical result in Eq. (17) with the quantum result in Eq. (9), we assume that  $\hat{B}$  and  $\hat{D}$  are in a two-mode squeezed coherent state, with squeeze parameter  $r$ . Then Eq. (9) can be written as

$$\langle\hat{\theta}_D(t)\hat{\theta}_{B1}(t_1)\rangle^2 + \langle\hat{\theta}_D(t)\hat{\theta}_{B2}(t_1)\rangle^2 = \frac{\eta}{2}I^2[\sinh r\delta(t-t_1)]^2. \quad (18)$$

To make a fair comparison between classical and quantum models, in Eq. (17), we assume that  $\tilde{I}_D = \tilde{I}_B = 1$  Hz and  $\langle\tilde{\delta}(t)\tilde{\delta}(t_1)\rangle = \mathfrak{D}\delta(t-t_1)$  with  $\mathfrak{D}$  as correlation strength. As  $\tilde{\delta}(t)$  is small, the maximum value of  $\mathfrak{D}$  is much less than one. In contrast, the  $\sinh r$  term in Eq. (18) increases exponentially with  $r$ , leading to quantum advantage. The smaller value of classical correlation can be compensated by increasing [47]  $\tilde{I}_B$  and  $\tilde{I}_D$ , but then the target can easily know [33] that it is being probed. Hence, the quantum advantage is more strongly present for small  $I_B$  and  $I_D$ , which is generally true with entangled photon generation schemes. The low intensity of the probe helps in finding the target stealthily or for imaging samples without exposing them to high optical power. Quantum mechanics ensures that the correlations in Eq. (12), Eq. (13), and Eq. (9) are sharply peaked (Dirac delta function). On the other hand, classical correlations in Eq. (17) must be made sufficiently sharp; otherwise, the target's distance can not be accurately estimated. Entanglement generally leads to quantum advantage as it has larger correlations [48, 49] than the classical correlations. Hence, quantum mechanics maximizes the target detection chances by creating sharper and larger correlations than its classical counterpart.

### 3 Conclusion

The quantum advantage in optical ranging is studied using a cross-correlated homodyne measurement scheme. The entanglement between the probe and the idler leads to unique correlations, which filter out the probe from the environmental background. This technique is immune to environmental noise as there is no correlation between idler and the environment. The target detection and ranging efficiency are independent of the entanglement field intensity. Hence, a large intensity of entangled fields is not

required to keep the quantum advantage. The target detection efficiency is proportional to the reflectivity of the target and intensity of the non-entangled reference fields in the homodyne. Hence, the low reflectivity of the target can be negated by increasing the intensity of the reference fields. All these advantages make the technique more efficient for ranging a low-reflective target immersed in a noisy environment. By heuristic arguments, we showed that the targets with reflectivity as small as  $2/I^2$  can be detected and ranged.

**Acknowledgments** The author, SD, thanks Yong Li for the discussion on the measurement scheme. MJW acknowledges support from the ARC Centre of Excellence for Engineered Quantum Systems (CE170100009).

**Disclosures** The authors declare no conflicts of interest.

**Data availability** No data were generated or analyzed in the presented research.

**Author contribution** SD formulated the problem. SD and MJW came up with the measurement scheme to solve the problem. GG is involved with comparing the quantum illumination results with the technique described in this manuscript.

## References

- [1] Seth Lloyd. Enhanced sensitivity of photodetection via quantum illumination. *Science*, 321(5895):1463–1465, 2008.
- [2] ED Lopaeva, I Ruo Berchera, Ivo Pietro Degiovanni, S Olivares, Giorgio Brida, and Marco Genovese. Experimental realization of quantum illumination. *Physical review letters*, 110(15):153603, 2013.
- [3] Ranjith Nair and Mile Gu. Fundamental limits of quantum illumination. *Optica*, 7(7):771–774, 2020.
- [4] Si-Hui Tan, Baris I Erkmen, Vittorio Giovannetti, Saikat Guha, Seth Lloyd, Lorenzo Maccone, Stefano Pirandola, and Jeffrey H Shapiro. Quantum illumination with gaussian states. *Physical review letters*, 101(25):253601, 2008.
- [5] Eylee Jung and DaeKil Park. Quantum illumination with three-mode gaussian state. *Quantum Information Processing*, 21(2):71, 2022.
- [6] Athena Karsa, Gaetana Spedalieri, Quntao Zhuang, and Stefano Pirandola. Quantum illumination with a generic gaussian source. *Phys. Rev. Res.*, 2:023414, Jun 2020.
- [7] Man-Hong Yung, Fei Meng, Xiao-Ming Zhang, and Ming-Jing Zhao. One-shot detection limits of quantum illumination with discrete signals. *npj Quantum Information*, 6(1):75, 2020.
- [8] Mark Bradshaw, Lorcán O. Conlon, Spyros Tserkis, Mile Gu, Ping Koy Lam, and Syed M. Assad. Optimal probes for continuous-variable quantum illumination. *Phys. Rev. A*, 103:062413, Jun 2021.
- [9] ShengLi Zhang, JianSheng Guo, WanSu Bao, JianHong Shi, ChenHui Jin, XuBo Zou, and GuangCan Guo. Quantum illumination with photon-subtracted continuous-variable entanglement. *Physical review A*, 89(6):062309, 2014.
- [10] De He, X. N. Feng, and L. F. Wei. Sensitive enhancement of cat state quantum illumination. *Opt. Express*, 31(11):17709–17715, May 2023.

- [11] Changsuk Noh, Changhyoup Lee, and Su-Yong Lee. Quantum illumination with definite photon-number entangled states. JOSA B, 39(5):1316–1322, 2022.
- [12] Su-Yong Lee, Yong Sup Ihn, and Zaeill Kim. Quantum illumination via quantum-enhanced sensing. Phys. Rev. A, 103:012411, Jan 2021.
- [13] Ashwith Varadaraj Prabhu, Baladitya Suri, and CM Chandrashekar. Hyperentanglement-enhanced quantum illumination. Physical Review A, 103(5):052608, 2021.
- [14] Hao Yang, Wojciech Roga, Jonathan D. Pritchard, and John Jeffers. Gaussian state-based quantum illumination with simple photodetection. Opt. Express, 29(6):8199–8215, Mar 2021.
- [15] Saikat Guha and Baris I. Erkmen. Gaussian-state quantum-illumination receivers for target detection. Phys. Rev. A, 80:052310, Nov 2009.
- [16] Quntao Zhuang, Zheshen Zhang, and Jeffrey H. Shapiro. Optimum mixed-state discrimination for noisy entanglement-enhanced sensing. Phys. Rev. Lett., 118:040801, Jan 2017.
- [17] Jonathan N Blakely. Quantum illumination with a parametrically amplified idler. Physics Letters A, 400:127319, 2021.
- [18] Yonggi Jo, Sangkyung Lee, Yong Sup Ihn, Zaeill Kim, and Su-Yong Lee. Quantum illumination receiver using double homodyne detection. Physical Review Research, 3(1):013006, 2021.
- [19] Sylvain Borderieux, Arnaud Coatanhay, and Ali Khenchaf. Estimation of the influence of a noisy environment on the binary decision strategy in a quantum illumination radar. Sensors, 22(13), 2022.
- [20] MuSeong Kim, Mi-Ra Hwang, Eylee Jung, and DaeKil Park. Is entanglement a unique resource in quantum illumination? Quantum Information Processing, 22(2):98, 2023.
- [21] Jeffrey H Shapiro and Seth Lloyd. Quantum illumination versus coherent-state target detection. New Journal of Physics, 11(6):063045, 2009.
- [22] Zheshen Zhang, Sara Mouradian, Franco NC Wong, and Jeffrey H Shapiro. Entanglement-enhanced sensing in a lossy and noisy environment. Physical review letters, 114(11):110506, 2015.
- [23] A. R. Usha Devi and A. K. Rajagopal. Quantum target detection using entangled photons. Phys. Rev. A, 79:062320, Jun 2009.
- [24] Shabir Barzanjeh, Saikat Guha, Christian Weedbrook, David Vitali, Jeffrey H Shapiro, and Stefano Pirandola. Microwave quantum illumination. Physical review letters, 114(8):080503, 2015.
- [25] Shabir Barzanjeh, Stefano Pirandola, David Vitali, and Johannes M Fink. Microwave quantum illumination using a digital receiver. Science advances, 6(19):eabb0451, 2020.



- [26] David Luong, CW Sandbo Chang, AM Vadiraj, Anthony Damini, Christopher M Wilson, and Bhashyam Balaji. Receiver operating characteristics for a prototype quantum two-mode squeezing radar. IEEE Transactions on Aerospace and Electronic Systems, 56(3):2041–2060, 2019.
- [27] R. Assouly, R. Dassonneville, T. Peronnin, A. Bienfait, and B. Huard. Quantum advantage in microwave quantum radar. Nature Physics, 19(10):1418–1422, 2023.
- [28] Gewei Qian, Xingqi Xu, Shun-An Zhu, Chenran Xu, Fei Gao, V. V. Yakovlev, Xu Liu, Shi-Yao Zhu, and Da-Wei Wang. Quantum induced coherence light detection and ranging. Phys. Rev. Lett., 131:033603, Jul 2023.
- [29] Thomas Gregory, P-A Moreau, Ermes Toninelli, and Miles J Padgett. Imaging through noise with quantum illumination. Science advances, 6(6):eaay2652, 2020.
- [30] Rongyu Wei, Jun Li, Weihao Wang, Songhao Meng, Baoshan Zhang, and Qinghua Guo. Comparison of snr gain between quantum illumination radar and classical radar. Opt. Express, 30(20):36167–36175, Sep 2022.
- [31] K. Muhammed Shafi, A. Padhye, and C. M. Chandrashekar. Quantum illumination using polarization-path entangled single photons for low reflectivity object detection in a noisy background. Opt. Express, 31(20):32093–32104, Sep 2023.
- [32] Phillip S. Blakey, Han Liu, Georgios Papangelakis, Yutian Zhang, Zacharie M. Léger, Meng Lon Iu, and Amr S. Helmy. Quantum and non-local effects offer over 40 db noise resilience advantage towards quantum lidar. Nature Communications, 13(1):5633, 2022.
- [33] Han Liu, Daniel Giovannini, Haoyu He, Duncan England, Benjamin J. Sussman, Bhashyam Balaji, and Amr S. Helmy. Enhancing lidar performance metrics using continuous-wave photon-pair sources. Optica, 6(10):1349–1355, Oct 2019.
- [34] Bhashyam Balaji and Duncan England. Quantum illumination: A laboratory investigation. In 2018 International Carnahan Conference on Security Technology (ICCST), pages 1–4. IEEE, 2018.
- [35] C. W. Sandbo Chang, A. M. Vadiraj, J. Bourassa, B. Balaji, and C. M. Wilson. Quantum-enhanced noise radar. Applied Physics Letters, 114(11):112601, 03 2019.
- [36] Duncan G. England, Bhashyam Balaji, and Benjamin J. Sussman. Quantum-enhanced standoff detection using correlated photon pairs. Phys. Rev. A, 99:023828, Feb 2019.
- [37] Yingwen Zhang, Duncan England, Andrei Nomerotski, Peter Svihra, Steven Ferrante, Paul Hockett, and Benjamin Sussman. Multidimensional quantum-enhanced target detection via spectrotemporal-correlation measurements. Phys. Rev. A, 101:053808, May 2020.
- [38] Lorenzo Maccone and Changliang Ren. Quantum radar. Physical Review Letters, 124(20):200503, 2020.

- [39] Maximilian Reichert, Roberto Di Candia, Moe Z Win, and Mikel Sanz. Quantum-enhanced doppler lidar. npj Quantum Information, 8(1):147, 2022.
- [40] Quntao Zhuang. Quantum ranging with gaussian entanglement. Physical Review Letters, 126(24):240501, 2021.
- [41] Ricardo Gallego Torromé. Quantum illumination with multiple entangled photons. Advanced Quantum Technologies, 4(11):2100101, 2021.
- [42] Zixin Huang, Cosmo Lupo, and Pieter Kok. Quantum-limited estimation of range and velocity. PRX Quantum, 2(3):030303, 2021.
- [43] Quntao Zhuang, Zheshen Zhang, and Jeffrey H Shapiro. Entanglement-enhanced lidars for simultaneous range and velocity measurements. Physical Review A, 96(4):040304, 2017.
- [44] Jonathan P. Dowling. Quantum optical metrology – the lowdown on high-n00n states. Contemporary Physics, 49(2):125–143, 2008.
- [45] K. Børkje, A. Nunnenkamp, B. M. Zwickl, C. Yang, J. G. E. Harris, and S. M. Girvin. Observability of radiation-pressure shot noise in optomechanical systems. Phys. Rev. A, 82:013818, Jul 2010.
- [46] Junxin Chen, Massimiliano Rossi, David Mason, and Albert Schliesser. Entanglement of propagating optical modes via a mechanical interface. Nature Communications, 11(1):943, Feb 2020.
- [47] Han Liu, Changhao Qin, Georgios Papangelakis, Meng Lon Iu, and Amr S. Helmy. Compact all-fiber quantum-inspired lidar with over 100 db noise rejection and single photon sensitivity. Nature Communications, 14(1):5344, 2023.
- [48] Mark Hillery, Ho Trung Dung, and Hongjun Zheng. Conditions for entanglement in multipartite systems. Phys. Rev. A, 81:062322, Jun 2010.
- [49] Mark Hillery and M. Suhail Zubairy. Entanglement conditions for two-mode states. Phys. Rev. Lett., 96:050503, Feb 2006.